Copeia 106, No. 3, 2018, 427–435

Improving Vertebrate Skeleton Images: Fluorescence and the Non-Permanent Mounting of Cleared-and-Stained Specimens

W. Leo Smith[1], Chesney A. Buck[1], Gregory S. Ornay[1], Matthew P. Davis[2], Rene P. Martin[1], Sarah Z. Gibson[2], and Matthew G. Girard[1]

Visualizing complex morphological features using digital photographs is often challenging in comparative anatomical studies. Progress in comparative anatomical studies has made substantive shifts through the development of new and improved methods for preparing specimens and visualizing characters. The advent of enzyme-cleared and bone-stained specimens revolutionized comparative anatomical studies in the middle of the 20th century. Continued refinement and improvement on these techniques combined with alternative approaches to visualization have allowed for more detailed investigations of vertebrate anatomy. One of the most difficult challenges remaining in comparative anatomy is accurately communicating morphological variation, and methodological improvements that refine the visual explanation are critical. Here we present two methods that simplify and improve the digital imaging of vertebrate skeletons and their components. First, fluorescence microscopy with alizarin-stained specimens is shown to help identify bony margins, facilitate the identification of skeletal elements in extant and fossil specimens, enhance the light alizarin staining of bone, and differentiate skeletal and soft tissues. Second, the non-permanent mounting of cleared-and-stained vertebrate specimens in a glycerine-gelatin matrix allows researchers to temporarily pose specimens for otherwise impossible scientific or artistic images. These two methods greatly improve researchers' ability to visualize vertebrate specimens or characters they are describing. The improved communication of critical anatomical variation through visual means facilitates the explanations demanded by evolutionary research, specifically, and biology, generally.

VERTEBRATE biologists have been studying comparative anatomy using alizarin-stained skeletons since the beginning of the 20th century (Hollister, 1934; Springer and Johnson, 2000; Hilton et al., 2015). Taylor (1967) revolutionized these studies by developing a trypsin-based method for the soft-tissue clearing of bone-stained vertebrates. Subsequent research and experimentation have improved the techniques associated with the clearing and staining of vertebrates by combining bone stains with cartilage stains (Wassersug, 1976; Dingerkus and Uhler, 1977; Taylor and van Dyke, 1985), nerve stains (Song and Parenti, 1995), and/or tendon stains (Torres and Ramos, 2016). In addition to techniques associated with the clearing and staining of vertebrates, researchers have also developed, improved, and used other visualization techniques such as x-ray computed tomography (e.g., Schaefer, 2003; Webb et al., 2006; Gignac and Kley, 2014), magnetic resonance imaging (e.g., Sepulveda et al., 2007; Chakrabarty et al., 2011; Graham et al., 2014), and calcein-staining of cartilage (Du et al., 2001). All of these methods have been developed in whole or in part because of the challenges associated with the discovery and description of complex anatomical features.

Herein, we describe two methods that improve the imaging of cleared-and-stained vertebrate anatomy: fluorescence imaging and the non-permanent mounting of wet skeletons. Connolly and Yelick (2010) first described the value of alizarin autofluorescence in studying skeletal development. Their study emphasized the use of fluorescence when examining minute skeletal elements without the need for dissection. Additionally, paleontologists have used various forms of photoluminescence to aid the identification of fossilized elements relative to the surrounding matrix (e.g., Kaye et al., 2015; Frese et al., 2017). Finally, many researchers have identified the presence of biofluorescence (e.g., Sparks et al., 2014; Taboada et al., 2017; Smith et al., 2018) or the ecological role of fluorescence (e.g., Gerlach et al., 2014; Gruber et al., 2016) in living vertebrates. We expand on the observations of these researchers to highlight the value of fluorescence for comparative vertebrate anatomists and systematists, specifically highlighting the use of fluorescence microscopy with alizarin-stained specimens to help identify bony margins, facilitate the identification of skeletal elements in extant and fossil specimens, enhance the light alizarin staining of bone, and differentiate skeletal and soft tissues. Further, we build off earlier work on the mounting of insect genitalia (Schawaroch and Li, 2007) to develop a method for the non-permanent mounting of cleared-and-stained vertebrate specimens in a glycerine-gelatin matrix that allows researchers to temporarily pose specimens for scientific or artistic preparations. Cleared-and-stained specimens are often preferred over dried skeletons because they allow specimens to be manipulated to assess functional considerations and because the transparency of the skeleton facilitates element positional assessment. One of the complications with cleared-and-stained specimens is that the removal of the specimen's musculature results in a flaccid specimen that will often collapse on itself. This flimsiness makes it difficult to nearly impossible to effectively visualize some characteristics because the specimen will sag due to gravity. This sagging often makes it difficult to hold a cleared-and-stained specimen stable to allow for high-quality z-stacked images from specific angles (e.g., rostral or caudal views). The glycerine-gelatin mounting medium described in this study overcomes these difficulties and facilitates the creation of digital images that include z-stacking. We are confident that these techniques will improve the quality of digital images of cleared-and-stained or fossil vertebrates for publications and presentations as well as occasionally facilitating the dissection, preparation, and examination of specimens.

[1] Biodiversity Institute, 1345 Jayhawk Boulevard, University of Kansas, Lawrence, Kansas 66045; Email: (WLS) leosmith@ku.edu. Send reprint requests to WLS.

[2] Department of Biological Sciences, St. Cloud State University, St. Cloud, Minnesota 56301.

Submitted: 9 April 2018. Accepted: 29 May 2018. Associate Editor: D. S. Siegel.

 DOI: 10.1643/CG-18-047 Published online: 20 August 2018

MATERIALS AND METHODS

We developed or expanded these methods primarily to prepare cleared-and-stained vertebrate specimens for digital imaging. These methods take particular advantage of previously cleared-and-stained specimens or fossil specimens, and the conditions described below are best viewed as temporary. Institutional abbreviations follow Sabaj (2016).

Equipment used for examining Recent and fossil vertebrates under fluorescence

Macro photographs documenting the anatomy of specimens were taken under white (or daylight LED) lighting using a Nikon D800 with an AF-S VR Micro-NIKKOR 105mm f/2.8G IF-ED lens or a Nikon D5300 with an AF-S DX Micro-NIKKOR 40mm f/2.8G lens that used a Porta-Trace/Gagne LED Light Panel for transmitted light and two variable-intensity Genaray SpectroLED Essential 365 Bi-Color LED lights for reflected light. Macro photographs generated under fluorescence were taken using the Nikon D800 with an AF-S VR Micro-NIKKOR 105mm f/2.8G IF-ED lens that used two NightSea BlueStar flashlights for transmitted light that were filtered through the Nikon light-shading plate from the Nikon SMZ-18 microscope.

White-light macro images were created by placing the specimen (in glycerine) on a pane of glass that was suspended approximately one inch above the Porta-Trace light panel that provided transmitted light while a pair of Genaray continuous-light arrays were positioned above and lateral to the specimen for reflected light. The images were taken with a small aperture (for increased depth of field) and were properly exposed by manual comparisons at many shutter speeds. In general, automatic exposure results in underexposed images because of the brightly lit background. Images under fluorescence were created by placing the specimen (in glycerine) on a pane of glass that was suspended approximately one inch above a sheet of black velvet. Two BlueStar flashlights were positioned above and lateral to the specimen for reflected light. Often a sheet of Rosco Cinegel #3025 filter was cut and taped together to make a light-diffusion cone that surrounded the specimen but did not interfere with view of the camera lens. The cone helped to diffuse the spotlighting from the flashlights to help make the lighting more uniform across the specimen. The Nikon light-shading plate from the Nikon SMZ-18 microscope was placed between the lens and the specimen to filter out unwanted light. The images were taken with a small aperture (for increased depth of field) and were properly exposed by manual comparisons at many shutter speeds. Fluorescent images typically require extremely long exposures.

Microscope images documenting the anatomy of specimens were taken under white (or daylight LED) lighting using a diversity of LED fiber-optic light sources with a Lumenera INFINITY2-5 digital CCD camera attached to a Nikon SMZ-18 stereomicroscope that has a P2-SHR plan apo 0.5x objective lens. Microscope images taken under fluorescent lighting were taken using the Nikon SMZ-18 stereomicroscope with a P2-EFLI epi-fluorescence attachment and either a P2-EFL GFP-B or P2-ELF RFP filter cube.

White-light microscope images were created by placing the specimen (in glycerine) on a microscope stand that included LED transmitted light and two to six fiber-optic LED light-source arms that were variously directed toward the specimen for reflected light. Often a sheet of Rosco Cinegel #3025 filter was cut and taped together to make a light-diffusion cone that surrounded the specimen but did not interfere with view of the microscope's objective lens. Images under fluorescence were created by placing the specimen (in glycerine) on a sheet of black velvet that rested on the microscope stand. The filter cubes include filters for both limiting the reflected light source and for filtering the image captured by the objective lens, so altering the lighting is simply a matter of choosing the appropriate filter cube for each image.

Images taken under white light and/or fluorescent lighting were used alone, manipulated, or combined in Adobe Photoshop. For several images, the digital image processing procedure known as z-stacking (or focus stacking) was performed in which multiple images taken at different focal distances were algorithmically combined to give a single composite image with a greater depth of field than any of the component source images. Helicon Focus was used to generate z-stacked images.

Frequently, images taken under different lighting regimes can be combined to augment the information available in a single image. There are a diversity of methods that can be employed and researchers are encouraged to experiment. In Supplemental Files 1 and 2 (see Data Accessibility), we provide detailed protocols for researchers interested in combining independent fluorescent images in the red and green channels for cleared-and-stained specimens to simultaneously emphasize bony and soft-tissue elements or for researchers interested in combining fluorescent images of fossils to make a mask for digitally removing the matrix surrounding fossil specimens to highlight the fossilized vertebrate.

Use of glycerine-gelatin matrix for the non-permanent mounting of cleared-and-stained specimens

To visualize cleared-and-stained specimens, the following procedure was used to stabilize wet skeletal material in a glycerine-gelatin matrix.

Step 1.—Follow your preferred methods for the clearing and staining of specimens (e.g., Dingerkus and Uhler, 1977).

Step 2.—Transfer specimen(s) to a 45% glycerine in distilled or deionized water solution (hereafter glycerine solution). Ensure that the specimen(s) or specimen component(s) such as gill arches are properly equilibrated by gently stirring or disturbing the glycerine solution periodically. This step can take over 24 hours as many collections store cleared-and-stained specimens in considerably higher concentrations of glycerine.

Step 3.—Prepare the mounting medium by warming a solution of 60 ml of distilled or deionized water to 65–70°C and adding 2.5 g of Knox™ gelatin to the water. Continuously stir this solution until the gelatin is completely dissolved. Slowly add 40 ml of concentrated glycerine into gelatin-water solution and stir. Once the gelatin-glycerine solution is completely mixed, slowly pour the 100 ml gelatin-glycerine solution into box, beaker, or mold (hereafter box). Ensure that the stirring and pouring do not introduce substantial bubbles into the box. If larger or smaller volumes are needed, simply increase or decrease the chemicals proportionally.

Step 4.—Once the temperature of the glycerine-gelatin solution in the box cools to 35–40°C, transfer the specimen or skeletal element from its glycerine solution to the glycerine-gelatin solution in the box.

Step 5.—Under a microscope, manipulate and hold the specimen with dissection tools until the glycerine-gelatin solution solidifies enough into a matrix to support the specimen as desired. Be sure to remove dissection equipment before the matrix completely solidifies to avoid adding imperfections or voids into the matrix. Alternatively, pin the specimen into a silicone mold or wax bottom box or prop the specimen up in a clear box with extruded clear acrylic rods until the matrix solidifies sufficiently to hold the specimen. Ideally, remove the pins or rods before the matrix solidifies completely to avoid imperfections in the matrix. Complete setting of the matrix can take more than eight hours at room temperature, but it can be sped up at this stage by placing the box temporarily in a refrigerator or freezer.

Step 6.—Examine or image specimen as desired. This imaging can either be done in the box they were embedded in or they can be removed/cut from larger boxes. If cutting out specimens, ensure that the surfaces to be visualized are flat for improved imaging. If many angles from one side of the specimen are desired, ensure that there is sufficient matrix surrounding the specimen for repeated trimming on the same general side (e.g., multiple trims on the rostral end of the matrix when taking head-on and 3/4 views of a lizard head). Please note that if there are artifacts on a surface of the matrix, these can be mitigated by allowing a brief flow of warm water on the embedded specimen for 7–15 seconds. If there are substantial artifacts within the matrix (e.g., retained pin voids), consider imaging the specimen under fluorescence or restarting this process.

Step 7.—For gelatin removal after imaging, place box or embedded specimen in a larger container of warm water or under gentle running water. After several minutes, gently manipulate the gelatin around the specimen with your finger or blunt dissecting tools to encourage the glycerine-gelatin to dissolve. Removing the matrix should not take significant time or require significant labor.

Step 8.—Transfer the specimen or anatomical component to 45% glycerine solution for eight or more hours.

Step 9.—Transfer the specimen through 45%, 60%, 75%, etc. glycerine solutions (step up) until the specimen is in the preferred final glycerine and thymol solution.

RESULTS AND DISCUSSION

Imaging under fluorescence for the examination of Recent and fossil vertebrates

Herein we present techniques for the improved visualization of alizarin-stained vertebrate skeletons when viewed under fluorescent light rather than under traditional white-light microscopy. A tremendous amount of detail can be observed with traditional white-light microscopy, but visualization under fluorescence can help to clarify minute anatomy, mitigate issues associated with the transparency of skeletal elements, enhance light alizarin staining, facilitate the identification of skeletal elements, and help differentiate various tissues or materials.

Clarifying minute anatomy.—As first noted by Connolly and Yelick (2010), the autofluorescence of bone-staining alizarin can help clarify skeletal anatomy when examining minute bony elements without the need for dissection. We further their observations by demonstrating the greater detail that can be observed when larger alizarin-stained specimens are viewed under fluorescent light as well. In particular, fluorescence imaging benefits from the specimen producing the light itself (i.e., the alizarin-red-stained skeleton emits red light after absorbing the higher energy green light). It is this "self-lighting" combined with the filtering of the green light by the associated filter cube or light-shading plate that provides the clarity of this technique. Because the only light that remains unfiltered is the red fluorescence (in the example of alizarin red), it greatly improves the contrast and visibility of bone margins and sutures. As an example, we present a dorsal image of the head of a Plainfin Midshipman (*Porichthys notatus*). The white-light image (Fig. 1A, magnified in inset) shows, but mostly obscures, the unusual separation of the ascending process (arrow in Fig. 1A, B) of the premaxilla from the remainder of the premaxilla. In contrast, the fluorescent image (Fig. 1B, magnified in inset) highlights this unusual separation. Under white light, the separation between these two components of this bone is considerably less clear because of the transparency of the ascending process and the overlapping elements. Similarly, the margins of the pterotic in the Searcher (*Bathymaster signatus*) are considerably more visible under fluorescence when compared to the image taken under white light (Fig. 2A, C). Finally, the fluorescent imaging regime particularly shines when examining fossils where the fossilized minerals fluoresce relative to their surrounding matrix (e.g., †*Tanaocrossus kalliokoskii,* a †scanilepiform from the Chinle Formation). To emphasize the value of fluorescence in some fossils, we show the same microscopic image under three light regimes (white light [Fig. 2B], red fluorescence [Fig. 2D], and green fluorescence [Fig. 2F]) where the margins of the skeletons are clearly more visible under fluorescence (Fig. 2D, F). This distinction between the fossil and the matrix greatly facilitates the preparation of the fossil and the examination of the skeletal characteristics. For the fossil, we present a fourth image where the red and green fluorescent images have been combined and used as a mask (protocol in Supplemental File 1; see Data Accessibility) to "blackout" all of the matrix on the white-light image (Fig. 2B) to visualize only the fossilized specimen under white light (Fig. 2H). This use of fluorescent lighting or a combination of fluorescent and white lighting is particularly helpful for visualizing and illustrating fossil specimens and characters (Fig. 2H; Gibson, 2015, 2016; Ghedotti and Davis, 2016).

Enhancing light alizarin-red staining.—Many cleared-and-stained specimens are preferentially and purposefully lightly stained with alizarin red because it often benefits the examination of the thicker neurocranium, associated suspensorial elements, and vertebral column. Further, insufficient alizarin-red staining can result from poor fixation, excess decalcification from long-term storage in unbuffered formalin or too much time in acetic acid during alcian-blue staining, or too much exposure to light. Light alizarin-red staining often results in little to no staining of thinner items such as the median-fin supports and fin rays (Fig. 1C). This limited staining obscures character coding in the axial skeleton and median fins, in particular. Fluorescent lighting allows these lightly stained elements to be

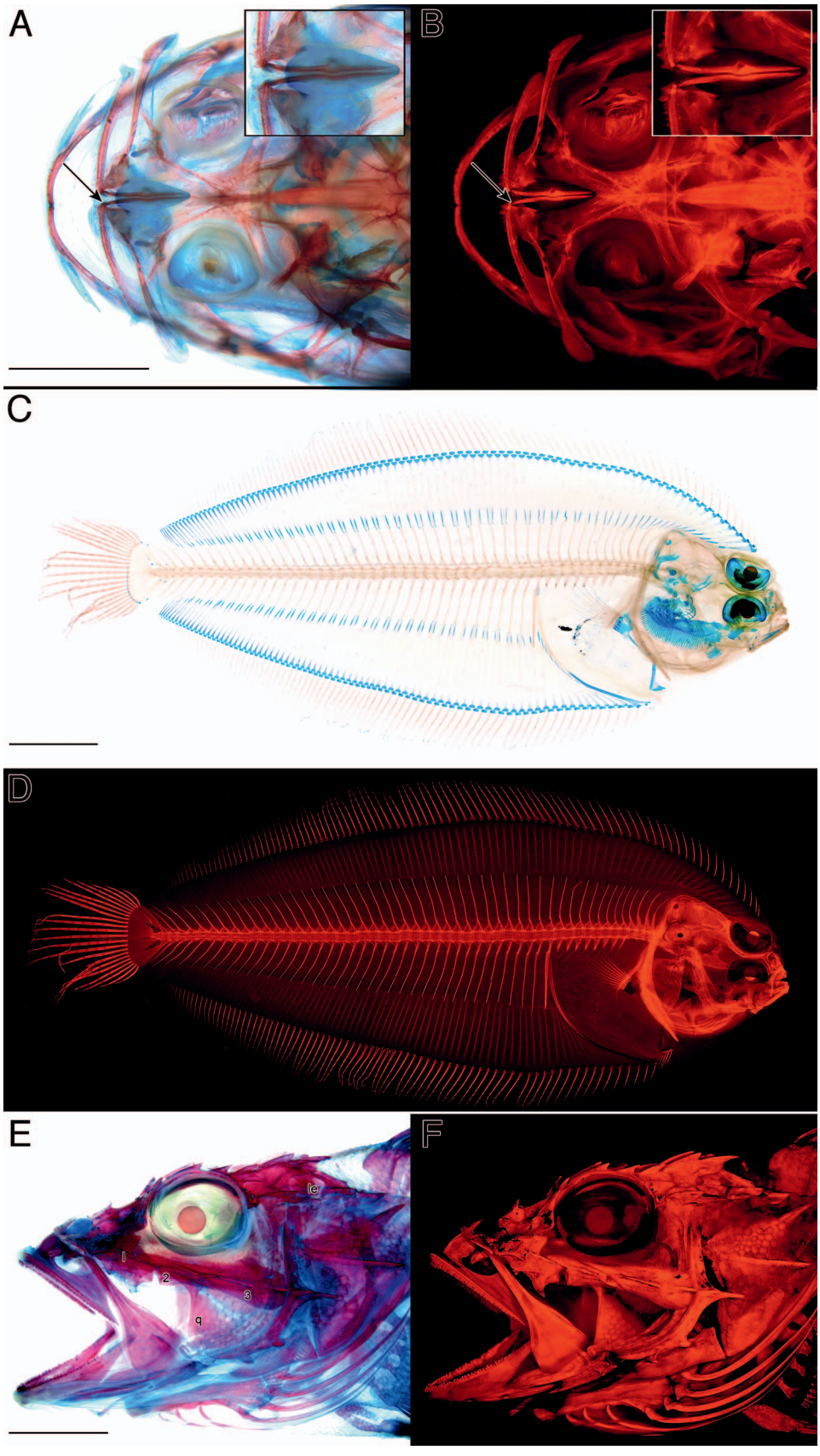

Fig. 1. Comparisons of cleared-and-stained fishes under white and fluorescent lighting. Dorsal view of the head of *Porichthys notatus* (KUI 18136) under (A) white and (B) fluorescent lighting highlighting the separation (arrows) of the ascending process of the premaxilla from the remainder of the bone. A magnified version of the separation is provided in the inset. Lateral view of *Lyopsetta exilis* (KUI 28289) under (C) white and (D) fluorescent lighting illustrating the value of fluorescence for "amplifying" lightly alizarin-red-stained bone. Lateral view of the head of *Neomerinthe hemingwayi* (AMNH 83911) under (E) white and (F) fluorescent lighting demonstrating the value of fluorescence for quickly recognizing skeletal-element limits. Scale bar is equal to 5 mm. Abbreviations: l = lachrymal, le = lateral extrascapular, q = quadrate, 2 = second circumorbital bone, and 3 = third circumorbital bone.

visualized because the visual amplification of bony elements under fluorescence makes these skeletal elements completely visible (Fig. 1D). The combination of fluorescent and white lighting allows these specimens to be completely coded for all characteristics.

Facilitating the identification of skeletal elements.—One of the benefits of examining and imaging specimens under fluorescence is that it facilitates the quick recognition of bone margins and the identification of distinct skeletal elements. As noted above, fluorescence illuminates as a

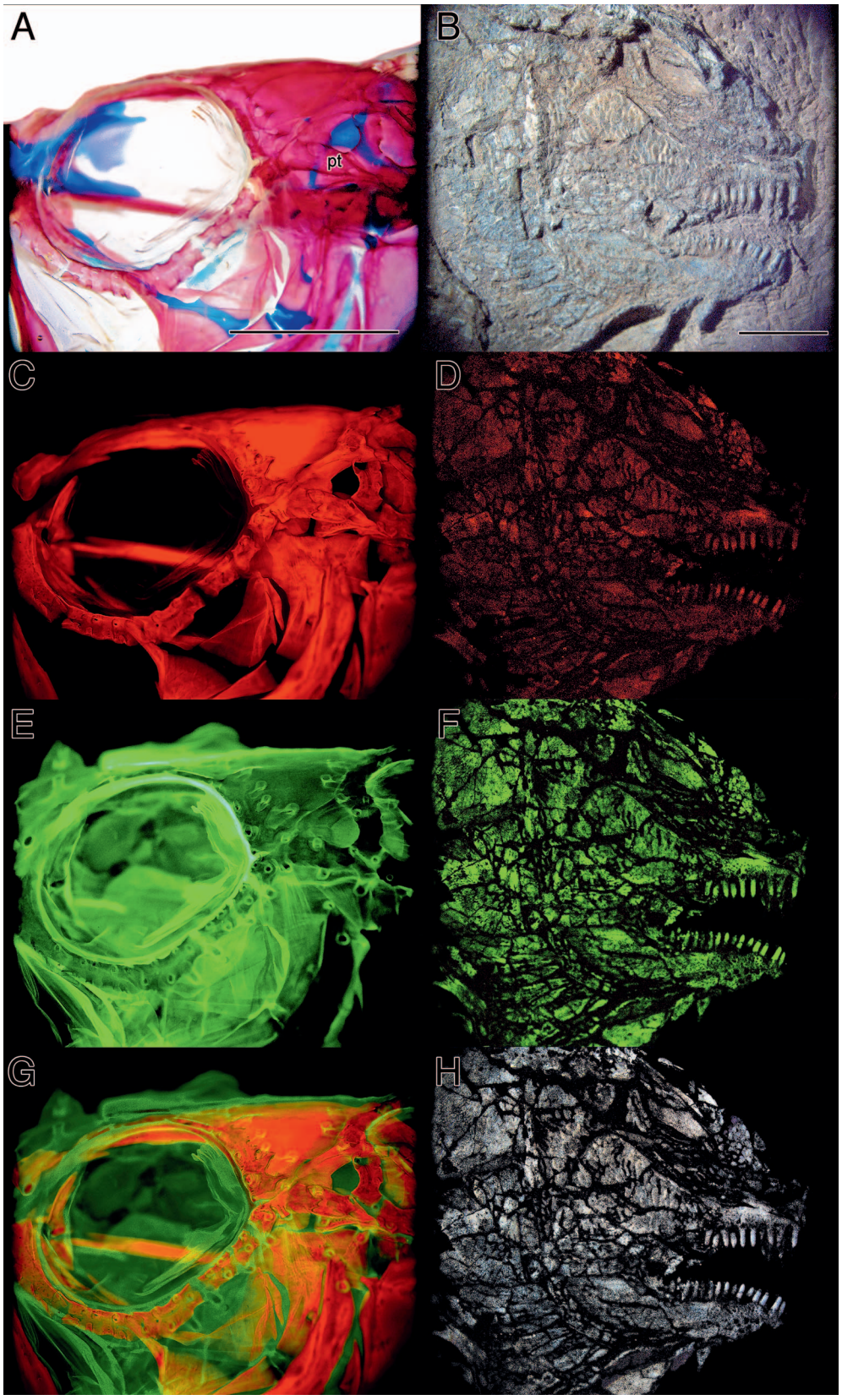

Fig. 2. Comparisons under different lighting regimes of a cleared-and-stained specimen of *Bathymaster signatus* (SIO 93-174; A, C, E, and G) and a fossilized specimen of †*Tanaocrossus kalliokoskii* (UMNH VP 22905; B, D, F, and H). The specimens are shown under (A–B) white lighting, (C–D) red fluorescence, and (E–F) green fluorescence. For the specimen of *Bathymaster*, these lighting regimes allow researchers to explore the relationship between soft-tissue and bony canals. This exploration is exemplified in the combined image (G) where the red fluorescent image is placed in the R channel and the green fluorescent image is placed in the G channel to combine these two images. For the specimen of †*Tanaocrossus,* these lighting regimes highlight the fluorescent fossil material relative to the non-fluorescent matrix (D, F). The images taken under white and fluorescent lighting can then be combined to illustrate the (H) fossilized material with the matrix removed by using the black areas of the fluorescent images as a mask to remove the matrix from the white light image. Scale bar is equal to 5 mm. Abbreviation: pt = pterotic.

reflection off of the specimens, so the alizarin-red-stained specimens produce the light. Because of this "self-illumination," the complications associated with the transparency of skeletons under traditional white-light examination are removed and the regions between bones completely lack light; these regions are simply not illuminated. As can be seen in the images of the Spinycheek Scorpionfish (*Neomerinthe hemingwayi*; Fig. 1E, F), fluorescence allows for the quick separation of the lachrymal and the second and third circumorbitals, which are not as clearly separated under white light. Similarly, the lateral extrascapular and quadrate margins are considerably more visible under fluorescence. This quick identification of elements is often helpful for imaging, but it can greatly aid the dissection of specimens

where bone limits can be critical for the clean separation of elements.

Differentiating tissues or materials.—In addition to the benefits of alizarin-red fluorescence, green fluorescence alone or in combination with red fluorescence can help highlight and differentiate different tissues. In the example of the Searcher (*Bathymaster signatus*), traditional white lighting (Fig. 2A) highlights the alcian-blue stained cartilage, and the transparency of elements allows the laterally incomplete lateral-line canals in the circumorbital bones to be easily recognized. The image under red fluorescence (Fig. 2C), as noted above, helps identify distinct skeletal elements, but the lack of transparency reduces the recognizable three-dimensionality of the circumorbital canals. The image under green fluorescence (Fig. 2E), in this case, highlights the lateral-line pores on the surface of the fish to some degree. In our experience, formalin-fixed specimens occasionally to often fluoresce green under blue lighting. This autofluorescence will often make superficial characteristics such as these pores considerably more visible. Finally, we present a fourth image where the red and green fluorescent images have been placed into the R and G channels of the RGB image, respectively. By combining these images using the protocol described in Supplemental File 2 (see Data Accessibility), we are able to visualize the bony lateral-line canals in the alizarin-stained image along with the highlighted lateral-line pores in the skin under green fluorescence. This combination of fluorescent lighting regimes is particularly helpful for visualizing the lateral-line system on the heads of cleared-and-stained fishes.

Non-permanent mounting of cleared-and-stained specimens in glycerine-gelatin matrix

In order to identify a non-destructive and temporary mounting medium for imaging cleared-and-stained vertebrates, we compared various concentrations of glycerine, two gelling agents (agarose and gelatin), and a variety of preparation strategies (e.g., rapid cooling of mounting medium). None of the agarose mixtures that solidified (i.e., solutions with a sufficient inclusion of agarose to solidify) were sufficiently transparent for the proper visualization of cleared-and-stained specimens. As was noted by Schawaroch and Li (2007), agarose generally performs poorly when mounting specimens. In contrast, gelatin worked well and was easier to work with. We found that a 40% glycerine solution generally worked best. Solutions with greater than 50% glycerine did not solidify as well and were difficult to work with because of the notable malleability and "wetness" of the resulting matrix. Solutions that were lower than 30% glycerine were less transparent and did not support the specimens well enough as the gel solidified. As the concentration of gelatin is increased in the solution, it browns, which decreases the clarity of the mounting medium but speeds up the gelling process. Minimizing gelatin is generally preferable. Using fewer than 2.0 g of gelatin per 100 ml of 40% glycerine solution resulted in a poorer mounting medium because it often gelled incompletely or not at all. The recommended recipe of 2.5 g gelatin in 100 ml of 40% glycerine resulted in a mounting medium that was sufficiently clear for imaging and gelled completely and at a pace that facilitated staging the specimen as it cooled. Many variations in gelling were attempted from placing the box in a refrigerator to placing the box on ice as the solution gelled. Once the matrix was set, placing the specimen in a freezer or refrigerator facilitated hardening; however, cooling the matrix before initial gelling often resulted in poorer mounts because bubbles were more often trapped in the medium as it cooled faster. These small bubbles form in all mixtures, but the prolonged gelling period allows more bubbles to escape.

For optimal results, be sure that cleared-and-stained specimens are transferred to 45% glycerine before embedding. With this concentration, the specimen will be approximately neutrally buoyant with the glycerine-gelatin solution which limits the speed that the specimen sinks to the bottom of the box and ensures that the specimen does not float. We experimented with a diversity of elements to position specimens as they harden. Whole specimens or elements are difficult to image if the specimen is resting on any surface that will be visible in the image. If embedding the specimens using silicone molds/boxes, we have had success piercing the silicone mold with pins to create a platform for the specimen to be held above the bottom of the box. If embedding the specimens using plastic boxes or other impenetrable containers, we recommend two alternative strategies. First, we recommend manually holding the specimen with forceps as the matrix hardens and then removing the forceps as soon as the specimen is stable but before the matrix fully hardens. This can take up to an hour using the standard recipe. Alternatively, we recommend the use of small pieces or rods of extruded clear acrylic to create platforms for "floating" the specimen above the bottom of the box. These nearly transparent rods can either be removed right before the matrix hardens (but after the matrix is stable), or they can be retained in the matrix and removed digitally using graphics software. While these rods are similar to the clarity of the matrix, they are not identical, so they will have to be removed digitally for optimal images if they are retained in the matrix.

Longevity and stability of mounting medium.—Specimens are relatively safe and stable for days to weeks in the temporary matrix. The matrix, if exposed to air, will form small pits on its surface that can be mitigated with short-term exposure to mildly warm water. During the development of this procedure, we have kept eight specimens in the matrix for over six months with three specimens in the matrix for over one year. During that time, one specimen that was kept in a non-airtight box developed modest fungal growth on the surface of the matrix after eight months of being embedded. We have not witnessed any other concerns with the technique or any signs of long-term damage from the embedding of specimens, but our recommendation is to remove the specimens from the matrix as soon at the images are complete or within one week of embedding to minimize the opportunities for specimen damage, particularly fungal growth.

Practical uses for the mounting of cleared-and-stained specimens in a glycerine-gelatin matrix.—Traditionally, many morphological features were difficult or impossible to image due to the flaccidity of cleared-and-stained specimens or because the specimens could not be held steady for z-stacking. The embedding procedure described here is a safe and low-cost method that facilitates the posing of cleared-and-stained specimens for complex biological or artistic presentations. Additionally, the value of being able to hold a specimen in place as you manipulate the hardened matrix to examine specimens from any angle cannot be understated

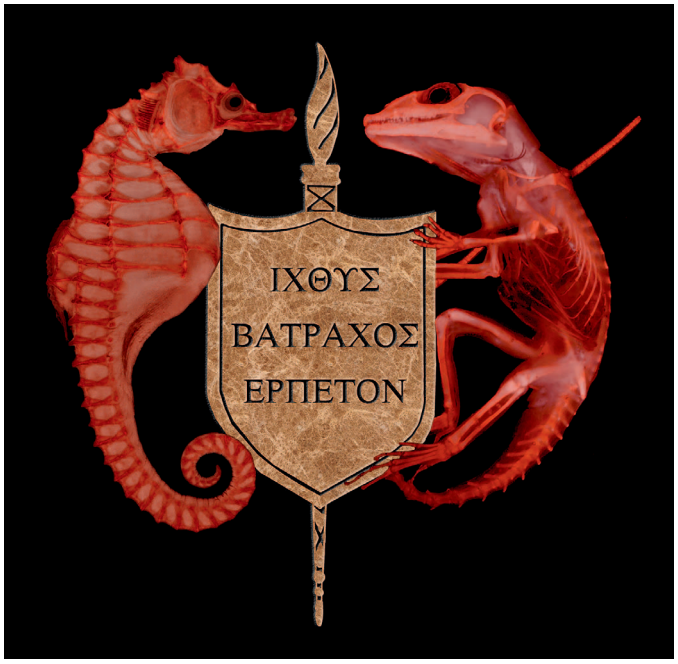

Fig. 3. American Society of Ichthyologists and Herpetologists logo re-created by embedding cleared-and-stained specimens of *Hippocampus erectus* (KUI 5107; left) and *Anolis* sp. (KUH uncat.; right) in a glycerine-gelatin matrix and imaging under fluorescence. The ASIH crest was added digitally.

when trying to observe, describe, or draw certain morphological features. To demonstrate the utility of this method, we present three use cases of glycerine-gelatin embedding.

First, we present a posed image of the Lined Seahorse (*Hippocampus erectus*) and an anole (*Anolis* sp.) that were combined with a digital image of the American Society of Ichthyologists and Herpetologists (ASIH) crest to generate a cleared-and-stained specimen version of the ASIH logo (Fig. 3). For this image, the two specimens were transferred from the glycerine solution to the glycerine-gelatin solution in a silicone-bottom box where they were pinned into position as the matrix solidified. Prior to the matrix completely hardening, the pins were removed. After the matrix hardened, the specimens were imaged with a digital camera with macro lens under fluorescent lighting to produce the final image.

Second, we present a head-on image of a Pacific Spiny Lumpsucker (*Eumicrotremus orbis;* Fig. 4). This image highlights how the matrix can add additional support, so that the cleared-and-stained vertebrate can be supported against gravity and be posed in a particular position (i.e., head-on with its mouth mildly open). To produce this image, we embedded the specimen in an 8-ounce glass jar and held the specimen in place with forceps as the matrix stabilized (approximately 40 minutes). After stabilization, the forceps were removed and the jar was placed in a freezer for 30 minutes to speed up matrix cooling. The specimen was imaged under fluorescence with a microscope (including the use of Helicon Focus for image stacking) and under white light with a digital camera without the use of image stacking. This image highlights the comparative strengths of fluorescence and traditional white-light microscopy. The image taken under fluorescence highlights the bony, alizarin-red-stained elements without the complications associated with transparency. The white-light images allow for the visualization of blue-stained cartilage (e.g., the diagnostic cartilaginous second and third basibranchials in the ventral gill arches of cyclopterids and liparids [Smith, 2005] visible through the mouth of the specimen) that are not visible under fluorescent lighting.

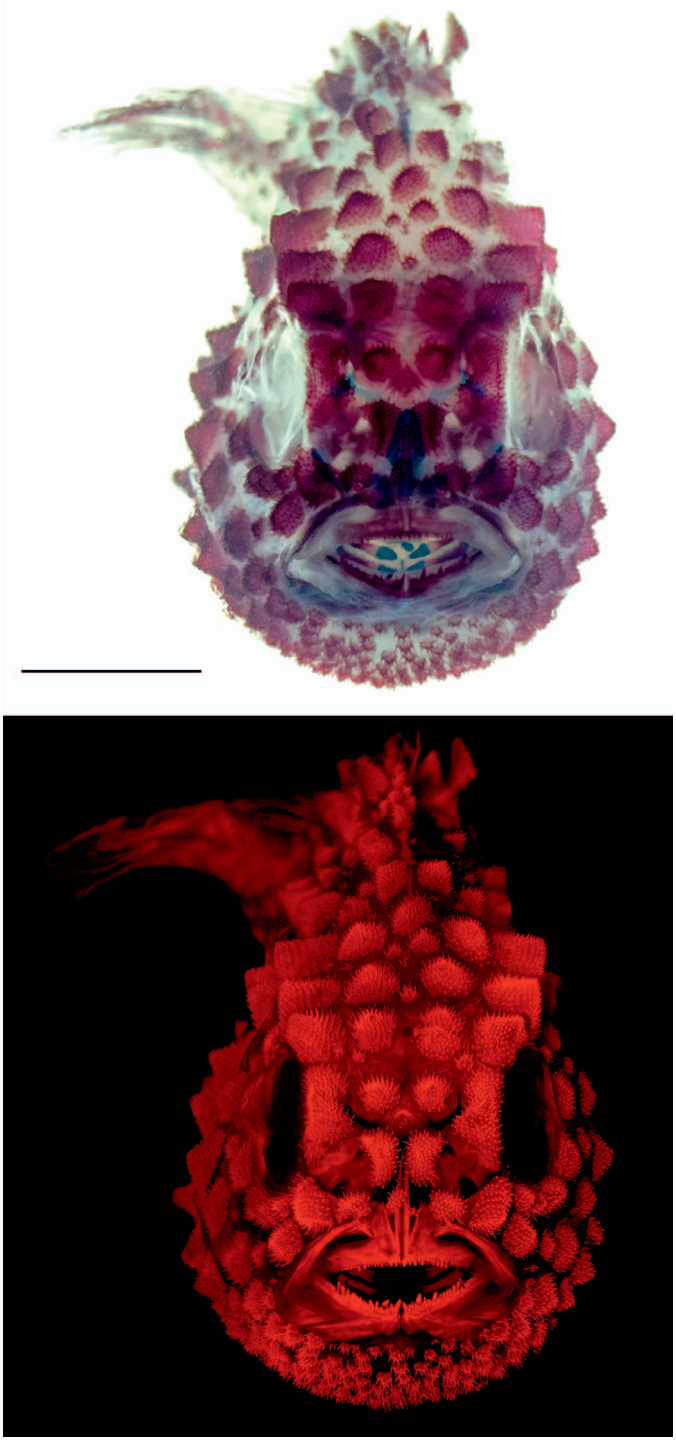

Fig. 4. Cleared-and-stained specimen of *Eumicrotremus orbis* (SIO 94-208) under white light (upper) and fluorescent light (lower). This specimen was embedded in a glycerine-gelatin matrix with the tail bent and mouth open to pose the specimen for a rostral view, which would be otherwise challenging due to the flaccidity of the specimen. Scale bar is equal to 5 mm.

Finally, we present images of a Florida Pompano (*Trachinotus carolinus*) where the specimen's gill arches were dissected and embedded in a small clear plastic box and

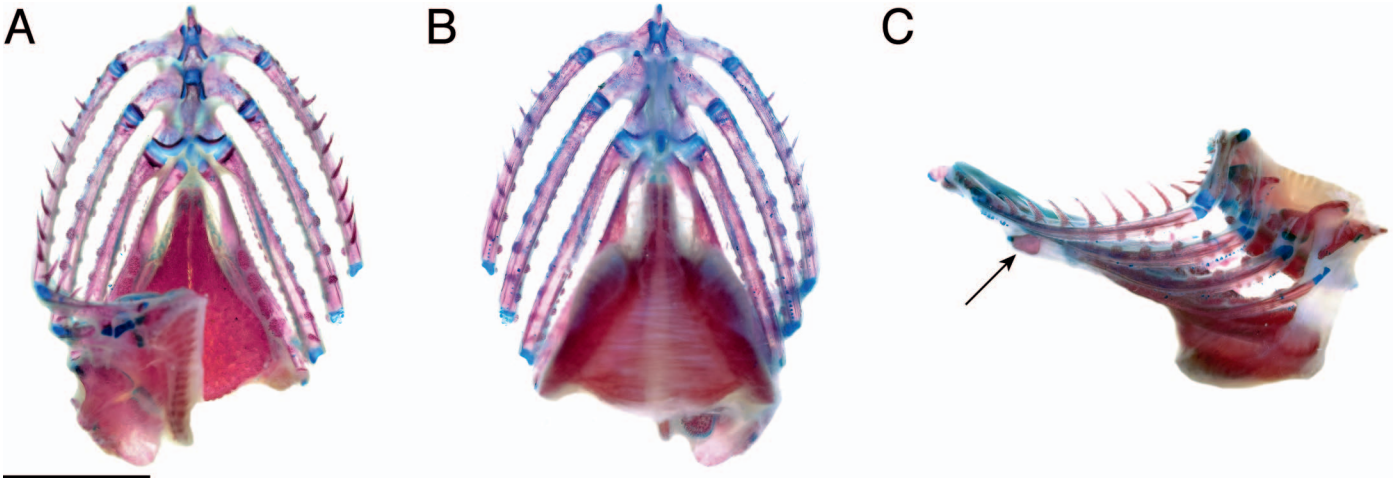

Fig. 5. Cleared-and-stained, glycerine-gelatin embedded gill arches (with right upper gill arches removed) of *Trachinotus carolinus* (KUI 20087) under white light from (A) dorsal, (B) ventral, and (C) lateral view highlighting the value of fixing the specimen in position, so it can be imaged from multiple angles. The arrow highlights the third hypobranchial process. Scale bar is equal to 5 mm.

imaged from multiple angles through the glycerine-gelatin matrix (dorsal image; Fig. 5A) or the plastic box (lateral and ventral images; Fig. 5A, B). The specimen was propped up with extruded clear acrylic rods that were removed before the matrix completely hardened. Images of the gill arches were taken under white light with a digital camera without image stacking. Traditionally, carangid ventral gill arches are viewed from a dorsal view or less commonly from a ventral view (e.g., Greenwood, 1976; Hilton et al., 2010). Unfortunately, these views can occasionally occlude or minimize the recognition of some phylogenetically informative characters. For example, when comparing the dorsal, ventral, and lateral views of the embedded gill arches, the rarely imaged lateral view highlights the third hypobranchial process that projects anteroventrally (arrow in Fig. 5C). Although this feature is visible in the ventral view, the three-dimensionality of the hypobranchial is obscured (Fig. 5B). The length, curvature, projections, and association of the third hypobranchials have been shown to be phylogenetically informative among carangiforms (Leis, 1994). The embedding of the gill arches in the glycerine-gelatin matrix allowed for the accurate, three-dimensional observation and imaging of this hypobranchial feature.

Conclusions.—The autofluorescence of alizarin-red highlighted in this study was recognized initially through an incidental examination of specimens under fluorescent lighting. We would highly recommend that researchers continue to explore the potential uses of specimen autofluorescence and the possibility that additional stains will fluoresce to improve specimen visualization. Further, a diversity of support structures were tested for gelatin embedding. Continued experimentation with the methods for pinning or holding specimens as the glycerine-gelatin mixture stabilizes are strongly encouraged.

MATERIAL EXAMINED

Anolis sp.: KUH uncatalogued

Bathymaster signatus: SIO 93-174

Eumicrotremus orbis: SIO 94-208

Hippocampus erectus: KUI 5107

Lyopsetta exilis: KUI 28289

Neomerinthe hemingwayi: AMNH 83911

Porichthys notatus: KUI 18136

†*Tanaocrossus kalliokoskii:* UMNH VP 22905

Trachinotus carolinus: KUI 20087

DATA ACCESSIBILITY

Supplemental material is available at http://www.copeiajournal.org/cg-18-047.

ACKNOWLEDGMENTS

We thank K. Smith for thoughtful discussions and editing drafts of this manuscript. We thank R. Arrindell, B. Brown, S. Schaefer, J. Sparks, and M. Stiassny (AMNH), A. Bentley, R. Brown, and L. Welton (KU), P. Hastings and H. Walker (SIO), and R. Irmis and C. Levitt-Bussian (UMNH) for access to specimens in their care. The research was funded by the University of Kansas and the National Science Foundation (NSF DEB-1543654). This investigation was supported by the University of Kansas General Research Fund allocation #2105077.

LITERATURE CITED

Chakrabarty, P., M. P. Davis, W. L. Smith, R. Berquist, K. M. Gledhill, L. R. Frank, and J. S. Sparks. 2011. Evolution of the light organ system in ponyfishes (Teleostei: Leiognathidae). Journal of Morphology 272:704–721.

Connolly, M. H., and P. C. Yelick. 2010. High-throughput methods for visualizing the teleost skeleton: capturing autofluorescence of alizarin red. Journal of Applied Ichthyology 26:274–277.

Dingerkus, G., and L. D. Uhler. 1977. Enzyme clearing of alcian blue stained whole small vertebrates for demonstration of cartilage. Biotechnic and Histochemistry 52:229–232.

Du, S. J., V. Frenkel, G. Kindschi, and Y. Zohar. 2001. Visualizing normal and defective bone development in

zebrafish embryos using the fluorescent chromophore calcein. Developmental Biology 238:239–246.

Frese, M., G. Gloy, R. G. Oberprieler, and D. B. Gore. 2017. Imaging of Jurassic fossils from the Talbragar Fish Bed using fluorescence, photoluminescence, and elemental and mineralogical mapping. PLoS ONE 12:e0179029.

Gerlach, T., D. Sprenger, and N. K. Michiels. 2014. Fairy wrasses perceive and respond to their deep red fluorescent coloration. Proceedings of the Royal Society of London B 281:20140787.

Ghedotti, M. J., and M. P. Davis. 2016. The taxonomic placement of three fossil *Fundulus* species and the timing of divergence within the North American topminnows (Teleostei: Fundulidae). Zootaxa 4250:577–586.

Gibson, S. Z. 2015. Evidence of a specialized feeding niche in a Late Triassic ray-finned fish: evolution of multidenticulate teeth and benthic scraping in †*Hemicalypterus*. The Science of Nature 102:10.

Gibson, S. Z. 2016. Redescription and phylogenetic placement of †*Hemicalypterus weiri* Schaeffer, 1967 (Actinopterygii, Neopterygii) from the Triassic Chinle Formation, southwestern United States: new insights into morphology, ecological niche, and phylogeny. PLoS ONE 11: e0163657.

Gignac, P. M., and N. J. Kley. 2014. Iodine-enhanced micro-CT imaging: methodological refinements for the study of the soft-tissue anatomy of post-embryonic vertebrates. Journal of Experimental Zoology Part B: Molecular and Developmental Evolution 322:166–176.

Graham, J. B., N. C. Wegner, L. A. Miller, C. J. Jew, N. C. Lai, R. M. Berquist, L. R. Frank, and J. A. Long. 2014. Spiracular air breathing in polypterid fishes and its implications for aerial respiration in stem tetrapods. Nature Communications 5:3022.

Greenwood, P. H. 1976. A review of the family Centropomidae (Pisces, Perciformes). Bulletin of the British Museum of Natural History 29:1–81.

Gruber, D. F., E. R. Loew, D. D. Deheyn, D. Akkaynak, J. P. Gaffney, W. L. Smith, M. P. Davis, J. H. Stern, V. A. Pieribone, and J. S. Sparks. 2016. Biofluorescence in catsharks (Scyliorhinidae): fundamental description and relevance for elasmobranch visual ecology. Nature: Scientific Reports 6:24751.

Hilton, E. J., G. D. Johnson, and W. F. Smith-Vaniz. 2010. Osteology and systematics of *Parastromateus niger* (Perciformes: Carangidae), with comments on the carangid dorsal gill-arch skeleton. Copeia 2010:312–333.

Hilton, E. J., N. K. Schnell, and P. Konstantinidis. 2015. When tradition meets technology: systematic morphology of fishes in the early 21st century. Copeia 103:858–873.

Hollister, G. 1934. Clearing and dyeing fish for bone study. Zoologica 12:89–100.

Kaye, T. G., A. R. Falk, M. Pittman, P. C. Sereno, L. D. Martin, D. A. Burnham, E. Gong, X. Xu, and Y. Wang. 2015. Laser-stimulated fluorescence in paleontology. PLoS ONE 10:e0125923.

Leis, J. M. 1994. Larvae, adults and relationships of the monotypic perciform fish family Lactariidae. Records of the Australian Museum 46:131–143.

Sabaj, M. H. (Ed.). 2016. Standard symbolic codes for institutional resource collections in herpetology and ichthyology: an Online Reference. Version 6.5 (16 August 2016). Electronically accessible at http://www.asih.org/, American Society of Ichthyologists and Herpetologists, Washington, D.C.

Schaefer, S. A. 2003. Relationships of *Lithogenes villosus* Eigenmann, 1909 (Siluriformes, Loricariidae): evidence from high-resolution computed microtomography. American Museum Novitates 3401:1–55.

Schawaroch, V., and S. C. Li. 2007. Testing mounting media to eliminate background noise in confocal microscope 3-D images of insect genitalia. Scanning 29:177–184.

Sepulveda, C. A., K. A. Dickson, L. R. Frank, and J. B. Graham. 2007. Cranial endothermy and a putative brain heater in the most basal tuna species, *Allothunnus fallai*. Journal of Fish Biology 70:1720–1733.

Smith, W. L. 2005. The limits and relationships of mail-cheeked fishes (Teleostei: Percomorpha) and the evolution of venom in fishes. Unpubl. Ph.D. diss., Columbia University, New York.

Smith, W. L., E. Everman, and C. Richardson. 2018. Phylogeny and taxonomy of flatheads, scorpionfishes, sea robins, and stonefishes (Percomorpha: Scorpaeniformes) and the evolution of the lachrymal saber. Copeia 106:94–119.

Song, J., and L. R. Parenti. 1995. Clearing and staining whole fish specimens for simultaneous demonstration of bone, cartilage, and nerves. Copeia 1995:114–118.

Sparks, J. S., R. C. Schelly, W. L. Smith, M. P. Davis, D. Tchernov, V. A. Pieribone, and D. F. Gruber. 2014. The covert world of fish biofluorescence: a phylogenetically widespread and phenotypically variable phenomenon. PLoS ONE 9:e83259.

Springer, V. G., and G. D. Johnson. 2000. Use and advantages of ethanol solution of alizarin red S dye for staining bone in fishes. Copeia 2000:300–301.

Taboada, C., A. E. Brunetti, F. N. Pedron, F. C. Neto, D. A. Estrin, S. E. Bari, L. B. Chemes, N. B. Lopes, M. G. Lagorio, and J. Faivovich. 2017. Naturally occurring fluorescence in frogs. Proceedings of the National Academy of Sciences of the United States of America 114:3672–3677.

Taylor, W. R. 1967. An enzyme method of clearing and staining small vertebrates. Proceedings of the United States National Museum 122:1–17.

Taylor, W. R., and G. C. van Dyke. 1985. Revised procedures for staining and clearing small fishes and other vertebrates for bone and cartilage study. Cybium 9:107–119.

Torres, M., and E. Ramos. 2016. A new method for staining ligaments and tendons of small vertebrates. Copeia 104: 708–711.

Wassersug, R. J. 1976. A procedure for differential staining of cartilage and bone in whole formalin-fixed vertebrates. Biotechnic and Histochemistry 51:131–134.

Webb, J. F., W. L. Smith, and D. R. Ketten. 2006. The laterophysic connection and swim bladder of butterflyfishes in the genus *Chaetodon* (Perciformes: Chaetodontidae). Journal of Morphology 267:1338–1355.